MDPI

Article

Taxonomy and an Updated Phylogeny of *Anomoloma* (Amylocorticiales, Basidiomycota)

Meng Zhou [1], Josef Vlasák [2], Masoomeh Ghobad-Nejhad [3], Young Woon Lim [4] and Yu-Cheng Dai [1,*]

1   Institute of Microbiology, School of Ecology and Nature Conservation, Beijing Forestry University, Beijing 100083, China; zhoumeng9612@bjfu.edu.cn
2   Biology Centre, Institute of Plant Molecular Biology, Czech Academy of Sciences, Branišovská 31, CZ-370 05 České Budějovice, Czech Republic; vlasak@umbr.cas.cz
3   Department of Biotechnology, Iranian Research Organization for Science and Technology (IROST), Tehran 3353-5111, Iran; ghobadnejhad@gmail.com
4   Institute of Microbiology, School of Biological Sciences, National University, Seoul 08826, Korea; ywlim@snu.ac.kr
*   Correspondence: yuchengdai@bjfu.edu.cn

Abstract: *Anomoloma* is a cosmopolitan poroid wood-decaying genus, belonging to the Amylocorticiales. During a study on polypores, two new species of *Anomoloma* were found in Eurasia, and they are described as *A. denticulatum* and *A. eurasiaticum*. To examine the phylogenetic relationships among species of *Anomoloma*, we analyzed nuclear ribosomal sequence data from the ITS regions and the LSU gene. The result demonstrates that *A. denticulatum* and *A. eurasiaticum* are independent species that belong to the *Anomoloma* genus. Both new species share the principal characteristics of the genus, but *Anomoloma denticulatum* is characterized by extensive white rhizomorphs spreading under the whole fruiting body, angular pores measuring 1–2 per mm, distinctly lacerate to dentate dissepiments and basidiospores of 3.5–4.3 × 2–2.5 μm. *Anomoloma eurasiaticum* is characterized by bearing plenty of large crystals on the mycelia and growth on *Picea* in high altitude areas. A key to the accepted species of *Anomoloma* worldwide is provided.

Keywords: phylogenetic analysis; Amylocorticiales; taxonomy; wood-rotting fungi

1. Introduction

Wood-inhabiting fungi are a phylogenetically diverse assemblage of macromycetes and comprise important components of woodlands and some other terrestrial ecosystems. Through their effective enzymatic systems causing wood decomposition, they play a crucial role in the global carbon and nutrient cycles [1,2]. Among the most significant groups of wood-inhabiting macromycetes are polypore fungi. The characterization of additional species in this group would improve our understanding of the decayer fungal community as a whole.

Anomoloma Niemelä & K.H. Larss. is a cosmopolitan wood-inhabiting fungal genus and its species cause a white rot in their wood substrata [3,4]. The genus is typified by *Anomoloma albolutescens* (Romell) Niemelä & K.H. Larss, and resides in the order Amylocorticiales, and the family Amylocorticiaceae. *Anomoloma* is distinguished from other similar genera by resupinate, soft, white, cream, or yellow basidiocarps with rhizomorphs, a monomitic hyphal structure with clamp connections, smooth and amyloid basidiospores, and causing a white rot on very rotten angiosperm and gymnosperm wood [3–5]. Previously, *Anomoloma* was treated as *Anomoporia* Pouzar due to their similar microscopic characteristics [6]. However, *Anomoloma* was separated from *Anomoporia* based on the wood decay type and molecular evidence, the former causing a white rot, while the latter causes a brown rot [5]. Four species were accepted when *Anomoloma* was established, and two species from subtropical China were described recently [4]. Currently, *Anomoloma*

accommodates six species worldwide: *A. albolutescens*, *A. flavissimum* (Niemelä) Niemelä & K.H. Larss., *A. myceliosum* (Niemelä) Niemelä & K.H. Larss., *A. rhizosum* Y.C. Dai & Niemelä, *A. luteoalbum* J. Song & B.K. Cui and *A. submyceliosum* J. Song & B.K. Cui.

Anomoloma has simple morphological structures; sometimes it is difficult to find characteristics to distinguish the species in the genus. Molecular phylogenies supply solid evidence to define species of the genus [4], a similar phenomenon has also been found in other polypores [7,8].

In the course of the exploration of polypores in the East Himalayan area of China, four white, and resupinate specimens were collected from Yunnan and Sichuan Provinces, and their morphological features, taxonomic affinities and phylogenetic relationships were analyzed. Combining these with samples collected from Europe and North America, the taxonomy and phylogeny of the genus here are updated. Two species are confirmed as new within *Anomoloma*, and they are simultaneously described and illustrated. In addition, an identification key to the accepted species of *Anomoloma* is provided.

2. Materials and Methods

2.1. Morphological Studies

The analyzed materials were preserved in the herbarium of the Beijing Forestry University (BJFC) in Beijing, China and the National Museum Prague of the Czech Republic (PRM). The macromorphology of the materials was determined according to our photographs in situ and the measurements of voucher materials. The micromorphological study followed Li et al. [9]. For the data on basidiospores, 5% of measurements treated at extreme measured values were excluded and are shown in parentheses. L = arithmetic average length of basidiospores, W = arithmetic average width of spores, Q = variation in the L/W ratios between the voucher specimens examined, n (a/b) = number of spores (a) measured from a given number (b) of specimens. Color terms refer to Petersen [10]. The herbarium code refer to Thiers [11].

2.2. DNA Extraction and Sequencing

A phylogeny based on the combined ITS and LSU DNA sequence data was analyzed with a total of 44 specimens including 20 species of Anomoloma related genera. A CTAB rapid plant genome extraction kit (Aidlab Biotechnologies Co., Ltd., Beijing, China) was applied in obtaining PCR products from dried materials, following the manufacturer's instructions with some adjustments [12]. To generate PCR amplicons, the following primer pair of ITS5 and ITS4 was used for the ITS (the internal transcribed spacer) region: ITS1, partial sequence; the 5.8S ribosomal RNA gene, complete sequence; and ITS2, partial sequence [13]. The primer pair for LR0R and LR7 was used for the LSU region (large subunit of nuclear ribosomal RNA gene) and included the 28S ribosomal RNA gene following Hopple and Vilgalys [14]. The PCR thermoprofile for different DNA sequences used in this study followed those used in Song et al. [4] The PCR procedure for ITS was as follows: initial denaturation at 95 °C for 3 min, followed by 34 cycles at 94 °C for 40 s, 54 °C for ITS and 72 °C for 1 min, and a final extension of 72 °C for 10 min. The PCR procedure for LSU was as follows: initial denaturation at 94 °C for 1 min, followed by 34 cycles at 94 °C for 30 s, 50 °C for 1 min and 72 °C for 1.5 min, and a final extension of 72 °C for 10 min. The PCR products were purified at the Beijing Genomics Institute (BGI), China. The purified products were then sequenced on an ABI-3730-XL DNA Analyzer (Applied Biosystems, Foster City, CA, USA). The quality of sequence was analysed following Nilsson et al. [15]. All new sequences were submitted to GenBank [16] and the related sequences of representative species were downloaded from GenBank, which belong to the target genus Anomoloma and allied genera (Table 1).

Table 1. Taxa, voucher specimens and GenBank accession numbers of sequences used in the phylogeny of *Anomoloma*.

Species	Specimen No.	Locality	GenBank Accessions		Reference
			ITS	LSU	
Amyloathelia crassiuscula	GB/K169-796	Sweden	DQ144610	DQ144610	[5]
Amylocorticium cebennense	HHB-2808	USA	GU187505	GU187561	[3]
A. cebennense	JS 24813	Norway	AY463376	AY586627	[17]
A. subincarnatum	AS 95	Sweden	AY463377	AY586628	[18]
A. subsulphureum	GB/M Ryberg	Sweden	DQ144611	DQ144611	[5]
A. subsulphureum	HHB-13817	USA	GU187506	GU187562	[3]
Amyloxenasma allantosporum	4527	Sweden	GU187498	GU187666	[3]
Anomoloma albolutescens	CFMR:L-6088	USA	GU187507	GU187563	[3]
A. albolutescens	H/RP 3549	Finland	DQ144612	DQ144612	[5]
A. albolutescens	Wei 2772	China	KT954951		[4]
A. albolutescens	LYBR 5671	France	ON053465[a]	ON038410[a]	
A. denticulatum	**Dai 23149**	**China**	**OM914148 [a]**	**OM914142 [a]**	
A. denticulatum	**Dai 23150**	**China**	**OM914149 [a]**	**OM914143 [a]**	
A. eurasiaticum	**Dai 22860**	**China**	**OM914144 [a]**	**OM914140 [a]**	
A. eurasiaticum	**Dai 22861**	**China**	**OM914145 [a]**		
A. eurasiaticum	**JV1108/4**	**Czechia**	**OM914147 [a]**	**OM914141 [a]**	
A. eurasiaticum	**H/TN 5911**	**Finland**	**DQ144614**		
A. flavissimum	H/TN 6397	China	DQ144613	DQ144613	[4]
A. flavissimum	Dai 2968a	China	KT954952	KT954966	[4]
A. flavissimum	Cui 10058	China	KT954953	KT954967	[4]
A. luteoalbum	Cui 2687	China	KT954961	KT954975	[4]
A. luteoalbum	Cui 8686	China	KT954962	KT954976	[4]
"*A. myceliosum*"	80	Russia	MK414515		GenBank
A. myceliosum	JV0509/42	USA	OM914150 [a]		
A. myceliosum	JV0509/117	USA	OM914151 [a]		
A. myceliosum	CFMR:MJL-4413	Canada	GU187500	GU187559	[3]
A. rhizosum	H/YD 4031	China	DQ144616	DQ144616	[5]
A. rhizosum	Cui 9717	China	KT954958	KT954972	[4]
A. rhizosum	Cui 10589	China	KT954959	KT954973	[4]
A. rhizosum	Cui 10618	China	KT954960	KT954974	[4]
A. sp.1	**JV0509/54**	**USA**	**OM914151 [a]**		
A. submyceliosum	Dai 7402	China	KT954963	KT954977	[4]
A. submyceliosum	Cui 2942	China	KT954965		[4]
Anomoporia bombycina	CFMR:L-6240	USA	GU187508	GU187564	[3]
A. bombycina	GGu612	Norway	AY463378	AY586629	[17]
A. kamtschatica	GB/M Edman K426	Sweden		DQ144615	[5]
A. kamtschatica	KHL11072	Sweden	AY463379	AY586630	[17]
A. vesiculosa	O/M Nunez 934	Japan	DQ144617	DQ144617	[5]
A. vesiculosa	Dai 5657	China	KT954949		[4]
A. vesiculosa	Cui 9523	China	KT954950		[4]
Hypochniciellum subillaqueatum	KHL 8493	Sweden	AY463431	AY586679	[17]
Podoserpula pusio	RH9929	New Zealand	KP191968	KP191769	GenBank
P. pusio	AFTOL-1522	Australia	DQ494688	DQ470821	[18]
P. pusio	H. Lepp 329	Australia	GU187555	EF535271	[3]

Bold: new taxa; [a]: new sequences; type material underlined.

2.3. Phylogenetic Analysis

The obtained sequences were aligned by BioEdit 7.0.5.3 [19]. After automatic alignment using Clustal X1.83 [20], the alignment was manually adjusted. The sequence alignment

and the tree file were uploaded to TreeBase (submission ID 29582). The sequence of *Hypochniciellum subillaqueatum* (Litsch.) Hjortstam downloaded from GenBank was used as an outgroup in the phylogenetic reconstruction of *Anomoloma* (Figure 1).
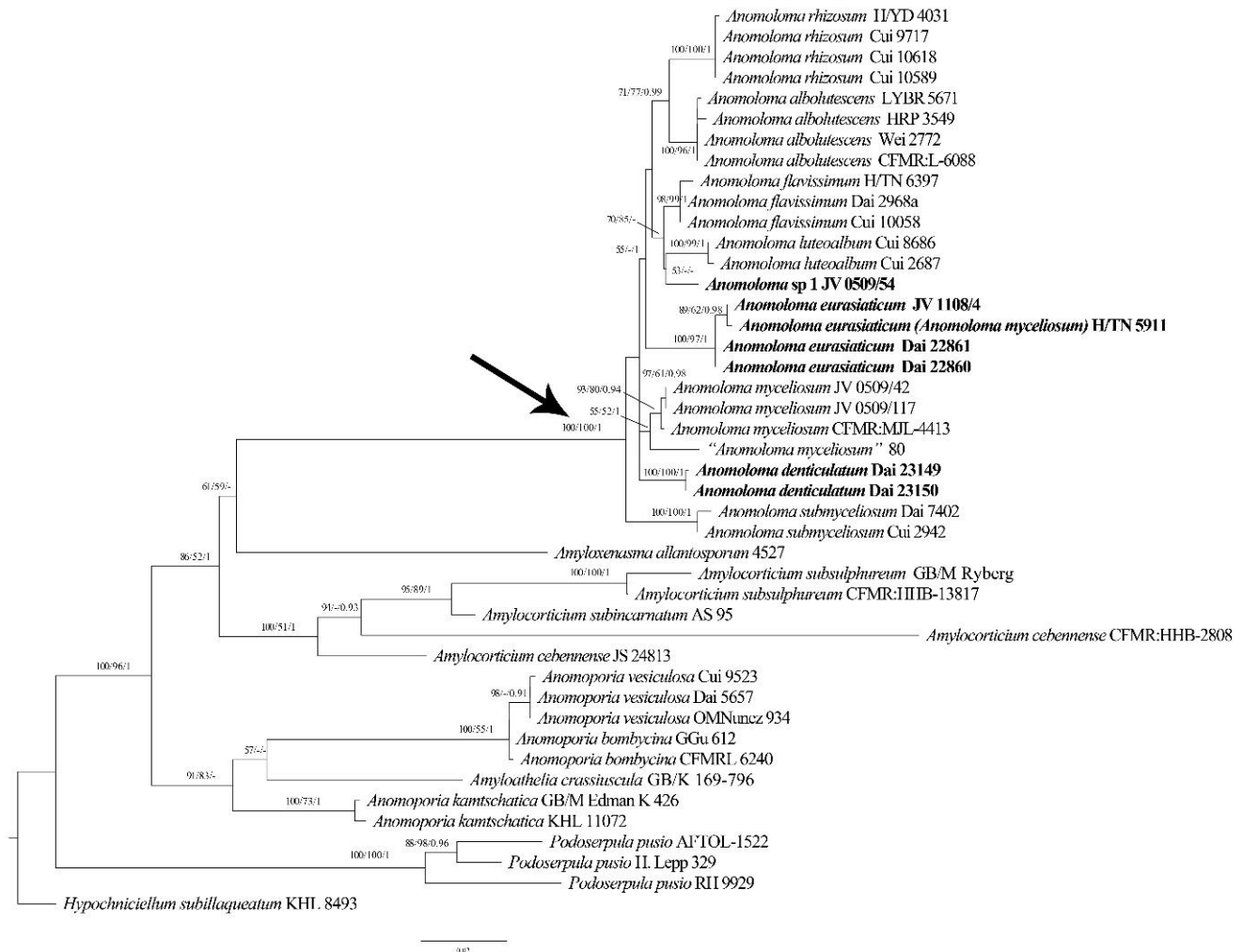

Figure 1. Maximum likelihood phylogenetic tree of *Anomoloma* species on the basis of ITS + LSU dataset. Branches are labeled with bootstrap values (MP/ML) >50%, and posterior probabilities (BI) > 0.90 respectively. New taxa are in bold. An arrow pointed the *Anomoloma* clade.

For the ultimate phylogenetic analyses, maximum parsimony (MP), maximum likelihood (ML) and Bayesian inference (BI) methods were utilized based on the ITS region and LSU sequence data. The three phylogenetic analysis algorithms outputted similar topologies to each other. Thus, the topology of the ML analysis is displayed as a representation with statistical values from the above three algorithms. The most parsimonious phylogenies were based on the combined ITS and LSU data, and their combinability was evaluated with the incongruence length difference (ILD) test [21] performed in PAUP* 4.0b10 [22]. The phylogenetic analysis approaches followed Zhao et al. [23]. The parsimony tree construction procedure was performed in PAUP* version 4.0b10 [22]. Trees were inferred using 100 replicates of the random stepwise addition of sequences and the tree-bisection reconnection (TBR) branch-swapping algorithm, with all characters given equal weight. The branch supports for all parsimony analyses were estimated by performing 1000 bootstrap (BT) replicates [24]. The descriptive tree statistics tree length (TL), consistency index (CI), retention index (RI), rescaled consistency index (RC), and homoplasy index (HI) were calculated for each maximum parsimonious tree (MPT) generated.

In the ML and BI analysis, jModeltest v.2.17 [25] was utilized to screen the best-fitting substitution model. Four unique partitions were established, and GTR + I + G was the selected substitution model for each partition. RaxmlGUI 1.2 [26,27] was applied in the ML analysis. All parameters in the ML analysis were kept at default settings. Statistical support values were obtained from non-parametric bootstrapping with 1000 replicates.

For the BI analysis implemented in MrBayes 3.2.6 [28], there were two independent runs—each of which had four chains for 2,000,000 generations sampling from the posterior distribution every 1000th generation to check that the PSRF (potential scale reduction factors) were reasonably close to 1.0 for all parameters indicative of chain convergence. The first 25% of the sampled trees were discarded as burn-in, while the remaining trees were used to obtain the Bayesian posterior probabilities (BPPs) of the clades.

The trees were shown in TreeView [29]. Branches that gained a bootstrap support for MP (BS) and ML(BP) values and BPPs (Bayesian posterior probabilities for BI) simultaneously of no less than 75% (BS/BP) and 0.95 (BPPs) were considered as significantly supported.

3. Results

3.1. Molecular Phylogeny

The combined ITS and LSU dataset contained 44 sequences representing 20 taxa. The dataset had an aligned length of 2083 characters including gaps (724 characters for ITS, 1359 characters for LSU), of which 1479 characters were constant, 197 were variable and parsimony-uninformative, and 407 were parsimony-informative. The MP analysis yielded 90 trees (TL = 1112, CI = 0.719, RI = 0.855, RC = 0.615, HI = 0.281). The best-fitting substitution model for the combined ITS + LSU dataset was evaluated and applied in the Bayesian analysis was GTR + I + G. The Bayesian analyses exported a nearly identical topology to the ML analyses with an average standard deviation of split frequencies = 0.009428. Both the BT values ($\geq$50%) and BPPs ($\geq$0.90) are displayed on the branches of the ML tree (Figure 1).

The resulting phylogenetic tree resolved a strongly supported *Anomoloma* clade and the newly sequenced taxa are nested in this clade. Judging from the molecular phylogenies, two new lineages of *Anomoloma* with robust support were identified. In addition, four samples of *Anomoloma eurasiaticum* formed an independent lineage with a robust support. JV 1108/4 and H/TN 5911 share the same ITS sequences, and the ITS sequences of Dai 22860 and Dai 22861 are identical, only two base pairs differences are found in the ITS regions between the former two and the latter two samples.

3.2. Taxonomy

Anomoloma denticulatum Y.C. Dai, Vlasák & Meng Zhou, sp. nov. Figures 2 and 3.
MycoBank: MB843478.

Diagnosis—*Anomoloma denticulatum* is characterized by a white pore surface with extensive white rhizomorphs spread under the whole fruiting body, angular pores measuring 1–2 per mm, distinctly lacerate to dentate dissepiments, ellipsoid basidiospores of 3.5–4.3 × 2–2.5 μm, and growth on decayed wood of *Abies* in the East Himalayan area.

Holotype—China, Sichuan, Luding County, Hailuogou National Forest Park, E 101°59′, N 29°35′, alt. 3050 m, on rotten wood of Abies, 8 October 2021, Yu-Cheng Dai, Dai 23150 (BJFC 037721).

Etymology—*Denticulatum* (Lat.): refer to the lacerate to dentate dissepiments of the species.

Description

Fruiting body—The basidiocarps are resupinate, annual, felty, soft corky, have no special odor or taste when fresh and dry, and are 11 cm × 4 cm and 0.2 mm thick. The sterile margin is distinct, snow-white, about 1 cm, radiciform and threadlike, with white rhizomorphs which extensively spread under the whole fruiting body, are visible in the poroid surface, and penetrate into rotten wood. The pores are cream when fresh and dry, angular, and 1–2(–3)/mm; dissepiments are rather thin, distinctly lacerate to dentate. The

subiculum is white when fresh and dry, felty, and about 0.1 mm thick. The tubes are white to cream when fresh and dry, soft corky, and about 0.1 mm long.

Figure 2. A basidiocarp of *Anomoloma denticulatum* (Dai 23150). Scale bar = 1.0 cm.

Hyphal structure—The hyphal system is monomitic; the clamped generative hyphae are neither amyloid nor dextrinoid in Melzer's reagent, and faintly cyanophilous in Cotton Blue; the tissues are unchanged in 5% potassium hydroxide.

Subiculum—The hyaline generative hyphae are slightly thick-walled with a wide lumen, smooth, frequently branched, flexuous, loosely interwoven, and 3–5 μm in diameter.

Tubes—The hyaline generative hyphae are thin- to slightly thick-walled with a wide lumen, frequently branched, flexuous, loosely interwoven, and 1.5–3 μm in diameter. Hyphae at the dissepiment edge are sometimes encrusted by fine and hyaline crystals. The basidia are clavate, bearing 4-sterigmata with a basal clamp connection, and 15–27 × 3.5–5 μm; the basidioles are of a similar shape but shorter.

Basidiospores—The basidiospores are oblong-ellipsoid to ellipsoid, hyaline, thin- to slightly thick-walled, smooth, amyloid in Melzer's reagent, acyanophilous, and (3.4−)3.5–4.3(−4.5) × 2–2.5(−2.7) μm, L = 3.84 μm, W = 2.15 μm, Q = 1.75–1.82 (n = 60/2).

Additional specimen (paratype) studied—China, Sichuan, Luding County, Hailuogou National Forest Park, E 101°59′, N 29°35′, alt. 3050 m, on rotten wood of *Abies*, 8 October 2021, Yu-Cheng Dai, Dai 23150 (BJFC 037720).

Anomoloma eurasiaticum Y.C. Dai, Vlasák & Meng Zhou, sp. nov. Figures 4 and 5.

MycoBank: MB843480.

Diagnosis—*Anomoloma eurasiaticum* is characterized by a white pore surface with rhizomorphs, angular pores measuring 3–5 per mm, oblong-ellipsoid to ellipsoid basidiospores of 3.2–4 × 2–2.8 μm, plenty of large crystals dispersed in mycelia, and growth on rotten gymnosperm wood in China and Europe.

Holotype—China, Yunnan, Deqin County, Baima Snow Mountain National Nature Reserve, E 98°50′, N 28°41′, alt. 3750 m, on rotten wood of *Picea*, 5 September 2021, Yu-Cheng Dai, Dai 22860 (BJFC 037433).

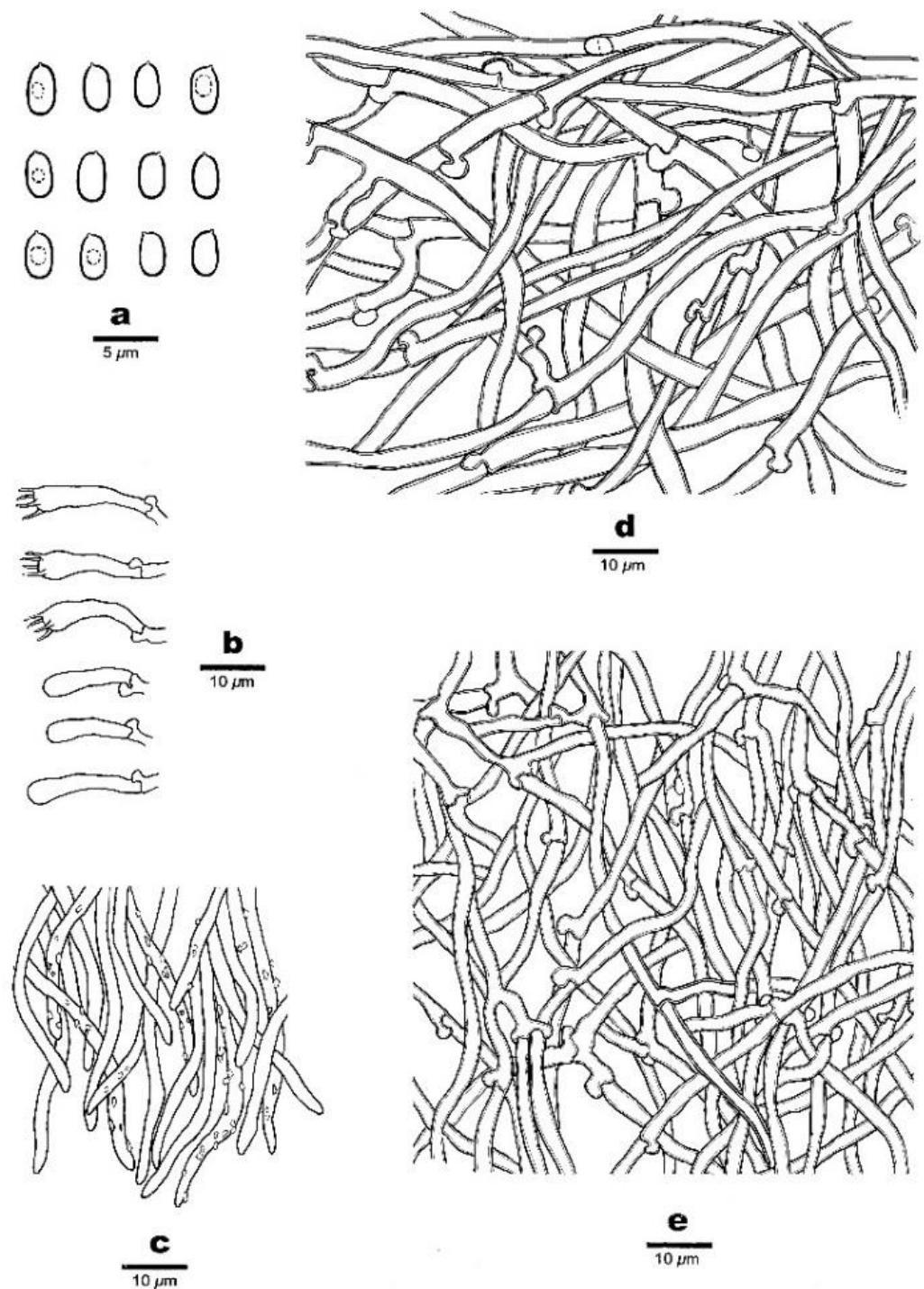Etymology—*Eurasiaticum* (Lat.): refer to a distribution in Eurasia.

Figure 3. Micro-morphology of *Anomoloma denticulatum* (Dai 23150). (**a**) Basidiospores. (**b**) Basidia and basidioles. (**c**) Hyphae at dissepiment edge. (**d**) A section of subiculum. (**e**) A section of trama.

Description

Fruiting body—The basidiocarps are resupinate, annual, felty, soft corky, of no special odor or taste when fresh and dry, 6 cm × 4 cm, and 0.3 mm thick. The sterile margin is distinct, snow-white, thinning out, about 0.5 cm, radiciform and threadlike, with white rhizomorphs which arise from the margin penetrating into rotten wood. The pores are white to cream when fresh, becoming cream to cream buff when dry, angular, and 3–5/mm; dissepiments are thin and slightly lacerate. The subiculum is white when fresh and dry,

felty, and about 0.1 mm thick. The tubes are white when fresh, cream when dry, soft corky, and about 0.2 mm long.

Figure 4. A basidiocarp of *Anomoloma eurasiaticum* (Dai 22860). Scale bar = 1.0 cm.

Hyphal structure—The hyphal system is monomitic; the clamped generative hyphae are neither amyloid nor dextrinoid in Melzer's reagent and faintly cyanophilous in Cotton Blue; tissues are unchanged in 5% potassium hydroxide.

Subiculum—The hyaline generative hyphae are slightly thick-walled with a wide lumen, frequently branched, flexuous, loosely interwoven, bearing plenty of fine crystals, and 2–3 μm in diameter.

Tubes—The hyaline generative hyphae are slightly thick-walled with a wide lumen, frequently branched, flexuous, loosely interwoven, 1.5–2.5 μm in diameter. The basidia are long, barrel-shaped, sometimes constricted at the middle, bearing 4-sterigmata and a basal clamp connection, and 13–20 × 3.5–5 μm; the basidioles are short clavate and shorter than basidia. Some large crystals present in the tube trama.

Basidiospores—The basidiospores are oblong-ellipsoid to ellipsoid, hyaline, thin- to slightly thick-walled, smooth, amyloid in Melzer's reagent, acyanophilous, and (3.1−)3.2–4(−4.1) × 2–2.8(−3) μm, L = 3.49 μm, W = 2.34 μm, Q = 1.42–1.50 (n = 90/3).

Additional specimen (paratype) studied: China, Yunnan, Deqin County, Baima Snow Mountain National Nature Reserve, E 98°50′, N 28°41′, alt. 3750 m, on rotten wood of *Picea*, 5 September 2021, Yu-Cheng Dai, Dai 22860 (BJFC 037434); Czechia, Hluboka, Libochovka, E 16°14′, N 49°23′, on rotten wood of *Picea*, August 2011, Josef Vlasák, JV1108/4 (PRM, duplicate, BJFC038577).
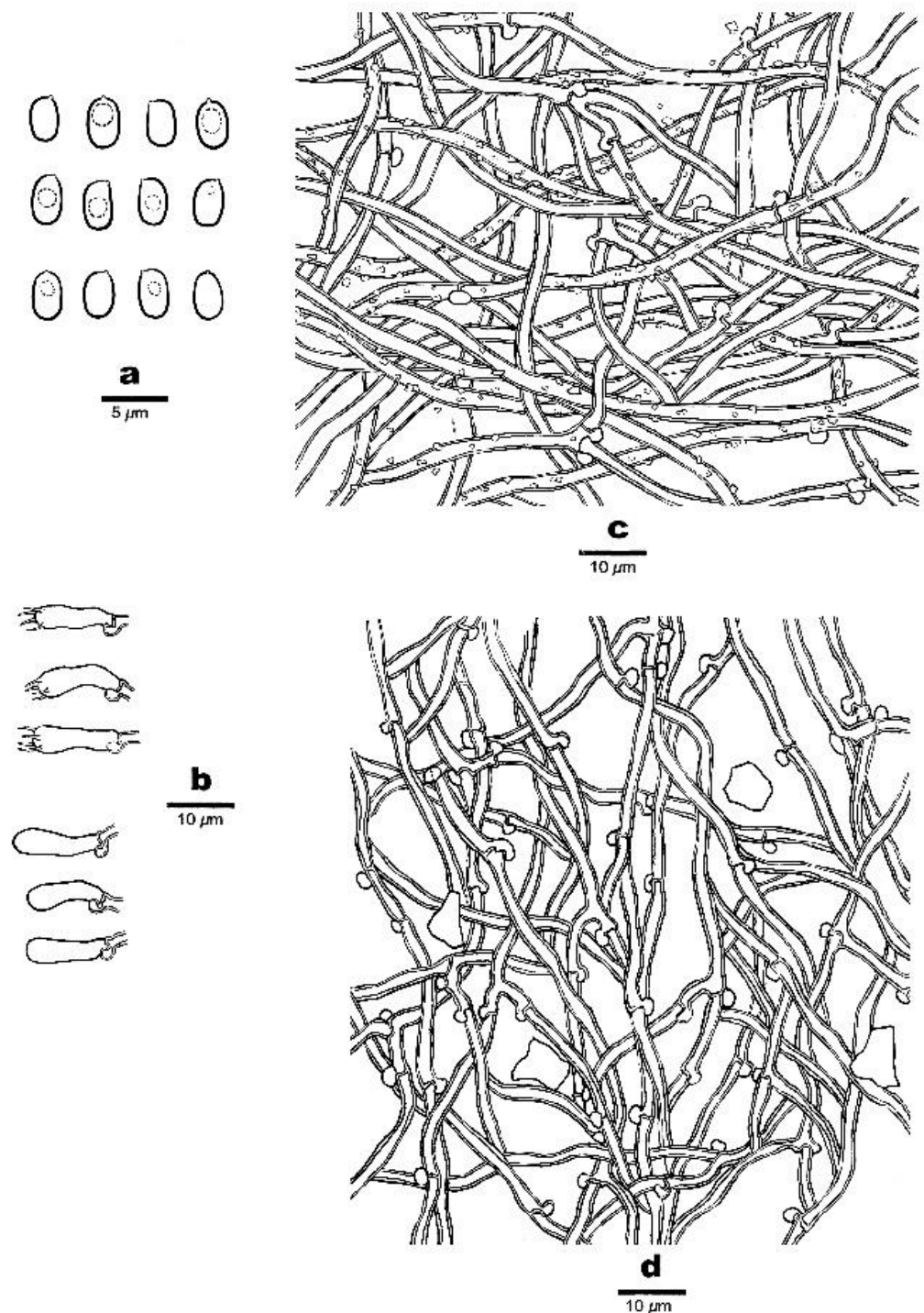
Figure 5. Micro-morphology of *Anomoloma eurasiaticum* (Dai 22860). (**a**) Basidiospores. (**b**) Basidia and basidioles. (**c**) A section of subiculum. (**d**) A section of trama.

4. Discussion

According to the phylogenetic analysis based on the ITS + LSU dataset, the mono-phyly of the genus *Anomoloma* was re-confirmed with robust supports (ML/MP = 100, BI = 1.00). Ten lineages representing ten taxa are nested in the *Anomoloma* clade (Figure 1). Two new species, *Anomoloma denticulatum* and *A. eurasiaticum*, form two well-supported linages within the *Anomoloma* clade. Interestingly the European and North American "*A. myceliosum*" are nested in two different linages. The type locality of *Anomoloma myceliosum* is North America, and the samples JV 0509/42 and JV 0509/117 from the USA and CFMR:

MJL-4413 from Canada most probably represent the real *A. myceliosum*. As Vlasák et al. [30] mentioned, the European "*Anomoloma myceliosum*" is probably a different species from the North American. In our study, the sample H/TN 5911 from Finland previously identified as *Anomoloma myceliosum* and sample JV1108/4 from Czechia are nested within the lineage of *A. eurasiaticum* with robust support. Thus, the samples of previously so-called *Anomoloma myceliosum* in Europe may represent *A. eurasiaticum*.

Sample 80, treated as "*Anomoloma myceliosum*", was collected in Altai in Russia. We failed to obtain the specimen, but it forms an independent linage and is closer to *A. myceliosum* (Figure 1). However, there is a 15-base-pair difference between the sequence of the Russian sample and the North American sample of *Anomoloma myceliosum*, which accounts for >2% of the nucleotides in the ITS regions. Thus, it is possible that another species of *Anomoloma* exists in Central Asia, but for the time being we treat this as "*Anomoloma myceliosum*".

Although the sample JV0509/54 from the USA forms an independent lineage within the *Anomoloma* clade in our phylogeny (Figure 1), it is temporarily treated as *Anomoloma* sp. 1 here because of the single sample. The taxon is characterized by a yellow pore surface with rhizomorphs spreading along the surface, angular, irregular pores of 3–4 per mm, a lack of cystidia and cystidioles, oblong-ellipsoid to ellipsoid basidiospores of 3.5–4 × 2.2–2.8 μm, and growth on the rotten wood of *Tsuga* in southeast USA.

On the basis of our study, the main characteristics of *Anomoloma* species are listed in Table 2.

In our phylogenetic analysis (Figure 1), *Anomoloma denticulatum* was nested in the *Anomoloma* clade as an independent lineage. Morphologically, *Anomoloma denticulatum* is similar to the white-pore species of *A. eurasiaticum*, *A. myceliosum*, and *A. submyceliosum*. However, *Anomoloma eurasiaticum* can be distinguished from *A. denticulatum* by its smaller pores (3–5/mm vs. 1–2/mm), slightly wider basidiospores (L = 3.49 μm, W = 2.34 μm, Q = 1.42–1.50 vs. L = 3.84 μm, W = 2.15 μm, Q = 1.78–1.82), and narrower subicular hyphae with minute hyaline crystals (2–3 μm vs. 3–5 μm). *Anomoloma myceliosum* is different from *A. denticulatum* in its wider basidiospores (L = 3.48 μm, W = 2.51 μm, Q = 1.34–1.46 vs. L = 3.84 μm, W = 2.15 μm Q = 1.78–1.82) and hyphae producing an oily substance with inconspicuous guttules [5,6]. In addition, the white rhizomorphs of *Anomoloma myceliosum* arise from the basidiocarp margin [5,6], but the rhizomorphs of *A. denticulatum* spread under the whole fruiting body. *Anomoloma submyceliosum* differs from *A. denticulatum* in its subicular hyphae covered with fine hyaline crystals, and its growth on angiosperm wood in subtropical areas [4].

Referring to the phylogenetic analysis of the ITS + LSU dataset, four samples of *Anomoloma eurasiaticum* form a well-supported lineage (ML = 100, MP = 97, BI = 1.00) within the *Anomoloma* clade. Morphologically, *Anomoloma eurasiaticum* may be recognized as *A. myceliosum* and *A. submyceliosum* by sharing a similar white-colored poroid surface. However, *Anomoloma myceliosum* differs from *A. eurasiaticum* in its ellipsoid or broadly ovate basidiospores (3–4.1 × 2.2–2.9 μm, Q = 1.34–1.46), bearing fragile, very thin-walled tramal hyphae and an oily hyphae tip with inconspicuous guttules [5,6]. *Anomoloma submyceliosum* can be differentiated from *A. eurasiaticum* by its larger pores (2–3/mm vs. 3–5/mm) and wider subicular hyphae (2.2–4.5 μm vs. 2–3 μm), and its growth on angiosperm wood in subtropical areas [4].

Previously, numerous macrofungi have been described from southwest China [31,32], and the present paper confirms that more undescribed wood-inhabiting fungi are present in the montane forests of the East Himalayas.

Other specimens studied: *Anomoloma myceliosum*. USA, Tennessee, Great Smoky Mt. on *Tsuga*, IX.2005, Josef Vlasák, JV0509/117 (dupl. BJFC038579); IX.2007, JV0509/42 (dupl. BJFC038581). *Anomoloma* sp 1. USA, Tennessee, Great Smoky Mt. on *Tsuga*, IX.2005, Josef Vlasák, JV0509/54 (dupl. BJFC038578).

Table 2. A morphological comparison of species in *Anomoloma*.

Species	Distribution (Type Locality Underlined)	Pore Surface	Sterile Margin	Rhizomorphs	Pore (per mm)	Tramal Hyphae	Subicular Hyphae	Cystidia and Cystidioles	Basidiospores (μm)	Hosts	References
A. albolutescens	China, Finland, <u>Sweden</u>, USA	cream to pale chrome yellow and distinctly yellow	thin, white or yellowish	yellow, spreading along surface	2–4	loosely subparallel	often covered with coarse or cubical crystals	absent	ellipsoid to subglobose, 3.9–5.2 × 2.9–3.6, L = 4.51, W = 3,25, Q = 1.36–1.46	gymnosperms, rarely angiosperms	[5,6]
A. denticulatum	China: <u>Sichuan</u>	cream	distinct, irregular	white, spreading under basidiocarp	1–2	interwoven	smooth	absent	oblong to ellipsoid, 3.5–4.3 × 2–2.5, L = 3.84, W = 2.15, Q = 1.75–1.82	*Abies*	This study
A. eurasiaticum	Czechia, China: <u>Yunnan</u>, Finland	white to cream and cream buff	irregular, white	white, spreading from margin	3–5	interwoven	often covered with minute hyaline crystals	absent	oblong to ellipsoid, 3.2–4 × 2–2.8, L = 3.49, W = 2.34, Q = 1.42–1.50	*Picea*	This study
A. flavissimum	China, <u>Russia</u>	bright chrome or sulphur yellow to vitelline	lemon yellow	yellow, spreading from margin	4–5	interwoven	often covered with coarse crystals.	present	ellipsoid or subglobose, 3.2–4.1 × 2.4–3.1, L = 3.66, W = 2.79, Q = 1.26–1.36	gymnosperms and very rotten wood of angiosperms	[5,6]
A. luteoalbum	China: <u>Zhejiang</u>	cream to yellowish	irregular, cream	yellow, spreading from margin	5–6	interwoven	often covered with minute hyaline crystals	absent	ellipsoid, 3–3.5 × 2–2.5, L = 3.2, W = 2.18, Q = 1.41–1.49	*Pinus*	[4]
A. myceliosum	Canada, <u>USA</u>	white to light cream	white, radially fibrous	white, extending deep into the substrate	3–4	interwoven	some hyphae covered with coarse crystals.	absent	ellipsoid or broadly ovate, with rounded ventral side, 3–4.1 × 2.2–2.9, L = 3.48, W = 2.51, Q = 1.34–1.46	gymnosperms, rarely angiosperms	[5,6]
A. rhizosum	China: <u>Sichuan</u>	yellowish to buff-yellow	irregular, yellow or ochraceous	straw–colored, spreading from margin	4–5	interwoven	rarely covered with minute hyaline crystals	absent	ellipsoid with truncated ends, 4.1–5.3 × 3–4, L = 4.82, W = 3.57, Q = 1.34–1.37	*Tsuga chinensis*	[5]
A. submyceliosum	China: <u>Fujian</u>	white to cream buff	irregular, white	white spreading from margin	2–3	interwoven	often covered with minute hyaline crystals	absent	ellipsoid, 3–4.2 × 2–2.7, L = 3.74, W = 2.32, Q = 1.54–1.69	angiosperm	[4]

Key to Accepted Species of Anomoloma

1 Pore surface and rhizomorphs white	5
1 Pore surface and rhizomorphs yellowish to yellow	2
2 Pores 2–4 per mm	*A. albolutescens*
2 Pores 4–6 per mm	3
3 Basidiospores usually >4 μm in length	*A. rhizosum*
3 Basidiospores usually <4 μm in length	4
4 Pore surface bright chrome or sulphur yellow; vesicular cystidia present	*A. flavissimum*
4 Pore surface cream to yellowish; vesicular cystidia absent	*A. luteoalbum*
5 Growth on angiosperm wood, occurrence in subtropical area	*A. submyceliosum*
5 Growth on gymnosperm wood, occurrence in temperate to boreal areas	6
6 Basidiospores ellipsoid or broadly ovate, Q = 1.34–1.46	*A. myceliosum*
6 Basidiospores oblong-ellipsoid to ellipsoid, Q >1.5	7
7 Pores 1–2 per mm, basidiospores Q = 1.75–1.82	*A. denticulatum*
7 Pores 3–5 per mm, basidiospores Q = 1.42–1.51	*A. crystallinum*

Data Availability Statement: Publicly available datasets were analyzed in this study. These data can be found here: (https://www.ncbi.nlm.nih.gov/; https://www.mycobank.org/page/Simple%20names%20search; http://purl.org/phylo/treebase, submission ID 29582) (accessed on 15 March 2022).

Conflicts of Interest: The authors declare no conflict of interest.

References

1. Rayner, A.D.M.; Boddy, L. Fungal decomposition of wood: Its biology and ecology. *Q. Rev. Biol.* **1988**, *73*, 1796–1803. [CrossRef]
2. White, N.A. The importance of wood-decay fungi in forest ecosystems: Fungal biotechnology in agriculture, food and environmental applications. In *Fungal Biotechnology in Agricultural, Food, and Environmental Applications*; Arora, D.K., Bridge, P.D., Bhatnagar, D., Eds.; Marcel Dekker: New York, NY, USA, 2003; pp. 375–392.
3. Binder, M.; Larsson, K.H.; Matheny, P.B.; Hibbett, D.S. Amylocorticiales ord. nov and Jaapiales ord. nov.: Early diverging clades of Agaricomycetidae dominated by corticioid forms. *Mycologia* **2010**, *102*, 865–880. [CrossRef] [PubMed]
4. Song, J.; Liu, X.Y.; Wang, M.; Cui, B.K. Phylogeny and taxonomy of the genus *Anomoloma* (Amylocorticiales, Basidiomycota). *Mycol. Prog.* **2016**, *15*, 11. [CrossRef]
5. Niemelä, T.; Larsson, K.H.; Dai, Y.C.; Larsson, E. *Anomoloma*, a new genus separated from *Anomoporia* on the basis of decay type and nuclear rDNA sequence data. *Mycotaxon* **2007**, *100*, 305–317.
6. Niemelä, T. Five species of *Anomoporia*, rare polypores of old forests. *Ann. Bot. Fenn.* **1994**, *31*, 93–115.
7. Yuan, Y.; Chen, J.J.; Korhonen, K.; Martin, F.; Dai, Y.C. An updated global species diversity and phylogeny in the forest pathogenic genus *Heterobasidion* (Basidiomycota, Russulales). *Front. Microbiol.* **2021**, *11*, 596393. [CrossRef]
8. Song, J.; Sun, Y.F.; Ji, X.; Dai, Y.C.; Cui, B.K. Phylogeny and taxonomy of *Laetiporus* (Basidiomycota, Polyporales) with descriptions of two new species from western China. *MycoKeys* **2018**, *37*, 57–71. [CrossRef]
9. Li, H.J.; Cui, B.K.; Dai, Y.C. Taxonomy and multi-gene phylogeny of *Datronia* (Polyporales, Basidiomycota). *Persoonia* **2014**, *32*, 170–182. [CrossRef]
10. Petersen, J.H. *The Danish Mycological Society's Colour-Chart*; Foreningen til Svampekundskabens Fremme: Greve, Denmark, 1996; pp. 1–6.
11. Thiers, B. *Index Herbariorum: A Global Directory of Public Herbaria and Associated Staff*; New York Botanical Garden's Virtual Herbarium: New York, NY, USA, 2018; Available online: http://sweetgum.nybg.org/science/ih/ (accessed on 15 March 2022).
12. Chen, J.J.; Cui, B.K.; Zhou, L.W.; Korhonen, K.; Dai, Y.C. Phylogeny, divergence time estimation, and biogeography of the genus *Heterobasidion* (Basidiomycota, Russulales). *Fungal Divers.* **2015**, *71*, 185–200. [CrossRef]
13. White, T.J.; Bruns, T.; Lee, S.; Taylor, J. Amplification and direct sequencing of fungal ribosomal RNA genes for phylogenetics. In *PCR Protocols: A Guide to Methods and Applications*; Innis, M.A., Gefand, D.H., Sninsky, J.J., White, M.J.T., Eds.; Academic Press: San Diego, FL, USA, 1990; pp. 315–322. [CrossRef]

14. Hopple, J.S.J.; Vilgalys, R. Phylogenetic relationships in the mushroom genus *Coprinus* and dark-spored allies based on sequence data from the nuclear gene coding for the large ribosomal subunit RNA: Divergent domains, outgroups, and monophyly. *Mol. Phylogenet. Evol.* **1999**, *13*, 1–19. [CrossRef]

15. Nilsson, R.H.; Tedersoo, L.; Abarenkov, K.; Ryberg, M.; Kristiansson, E.; Hartmann, M.; Schoch, C.L.; Nylander, J.A.A.; Bergsten, J.; Porter, T.M.; et al. Five simple guidelines for establishing basic authenticity and reliability of newly generated fungal ITS sequences. *MycoKeys* **2012**, *4*, 37–63. [CrossRef]

16. Sayers, E.W.; Cavanaugh, M.; Clark, K.; Pruitt, K.D.; Schoch, C.L.; Sherry, S.T.; Karsch-Mizrachi, I. GenBank. *Nucleic Acids Res.* **2022**, *50*, 161–164. Available online: https://www.ncbi.nlm.nih.gov/ (accessed on 15 March 2022). [CrossRef]

17. Larsson, K.H.; Larsson, E.; Kljalg, U. High phylogenetic diversity among corticioid homobasidiomycetes. *Mycol. Res.* **2004**, *108*, 983–1002. [CrossRef] [PubMed]

18. Matheny, P.B.; Curtis, J.M.; Hofstetter, V. Major clades of Agaricales: A multi-locus phylogenetic overview. *Mycologia* **2007**, *98*, 984–997.

19. Hall, T.A. Bioedit: A user-friendly biological sequence alignment editor and analysis program for Windows 95/98/NT. *Nucleic Acids Symp. Ser.* **1999**, *41*, 95–98.

20. Thompson, J.D.; Gibson, T.J.; Plewniak, F.; Jeanmougin, F.; Higgins, D.G. The CLUSTAL X windows interface: Flexible strategies for multiple sequence alignment aided by quality analysis tools. *Nucleic Acids Res.* **1997**, *25*, 4876–4882. [CrossRef]

21. Farris, J.S.; Mari, K.; Kluge, A.G.; Bult, C. Testing significance of incongruence. *Cladistics* **1994**, *10*, 315–319. [CrossRef]

22. Swofford, D.L. *PAUP*: PHYLOGENETIC Analysis Using Parsimony (*and Other Methods)*; Version 4.0b10; Sinauer Associates: Sunderland, MA, USA, 2002. [CrossRef]

23. Zhao, C.L.; Chen, H.; Song, J.; Cui, B.K. Phylogeny and taxonomy of the genus *Abundisporus* (Polyporales, Basidiomycota). *Mycol. Prog.* **2015**, *14*, 38. [CrossRef]

24. Felsenstein, J. Confidence intervals on phylogenetics: An approach using the bootstrap. *Evolution* **1985**, *39*, 783–791. [CrossRef]

25. Darriba, D.; Taboada, G.L.; Doallo, R.; Posada, D. jModelTest 2: More models, new heuristics and parallel computing. *Nat. Methods* **2012**, *9*, 772. [CrossRef]

26. Stamatakis, A. RAxML-VI-HPC: Maximum likelihood-based phylogenetic analysis with thousands of taxa and mixed models. *Bioinformatics* **2006**, *22*, 2688–2690. [CrossRef] [PubMed]

27. Silvestro, D.; Michalak, I. RaxmlGUI: A Graph. Front-End RAxML. *Org. Divers. Evol.* **2012**, *12*, 335–337. [CrossRef]

28. Ronquist, F.; Teslenko, M.; van der Mark, P.; Ayres, D.L.; Darling, A.; Hőhna, S.; Larget, B.; Liu, L.; Suchard, M.A.; Huelsenbeck, J.P. MrBayes 3.2: Efficient Bayesian phylogenetic inference and model choice across a large model space. *Syst. Biol.* **2012**, *61*, 539–542. [CrossRef] [PubMed]

29. Page, R.D.M. TreeView: Application to display phylogenetic trees on personal computers. *Comput. Appl. Biosci. Cabios* **1996**, *12*, 357–358. [CrossRef]

30. Vlasák, J.; Vampola, P.; Kout, J. New record of *Anomoloma* myceliosum in the Czech Republic. *Mykol. Listy* **2012**, *119*, 1–5.

31. Dai, Y.C.; Yang, Z.L.; Cui, B.K.; Wu, G.; Yuan, H.S.; Zhou, L.W.; He, S.H.; Ge, Z.W.; Wu, F.; Wei, Y.L.; et al. Diversity and systematics of the important macrofungi in Chinese forests. *Mycosystema* **2021**, *40*, 770–805. [CrossRef]

32. Wang, K.; Chen, S.L.; Dai, Y.C.; Jia, Z.F.; Li, T.H.; Liu, T.Z.; Phurbu, D.; Mamut, R.; Sun, G.Y.; Bau, T.; et al. Over-view of China's nomenclature novelties of fungi in the new century (2000–2020). *Mycosystema* **2021**, *40*, 822–833. [CrossRef]